NORSAR

NORSAR Scientific Report No. 2-98/99

Semiannual Technical Summary

1 October 1998 - 31 March 1999

Kjeller, May 1999

6.3 Monitoring of the European Arctic Using Regional Generalized Beamforming

Introduction

Since 1 January 1991 the Generalized Beamforming algorithm (GBF) has been running at NORSAR to provide automatic phase associations and event locations from the detection data of the regional arrays (Ringdal and Kværna, 1989). As of February 1999, data from NORES, ARCES, FINES, HFS, GERES, and the Apatity array were jointly processed, using a grid system as shown in Fig. 6.3.4.

In order to efficiently include data from the array at Spitsbergen (SPITS), there was a need to revisit both the signal processing of the individual arrays and the GBF software with respect to functionality, parameter setting and operational stability. The station locations and the new grid system is shown in Fig. 6.3.6. Different from the other arrays recorded at NORSAR, SPITS is located close to a region with relatively high natural seismicity. In addition, the glaciers and mines of Spitsbergen occasionally create a very large number of signals (several thousand per day) which creates problems for both the signal processing (DP/EP) and the automatic phase association process (GBF).

In this contribution, we will first summarize the improvements made to the signal processing of the different regional arrays. This will be followed by a description of the enhancements made to the GBF method. Finally we will illustrate the overall effects of the changes made, in particular resulting in a much improved monitoring capability for the European Arctic.

Improved detector and f-k recipes

During the last years several improvements in the automatic data processing for the regional arrays were developed. These new f-k recipes and detector modifications are since 10 April 1999 implemented in the daily routine analysis at NORSAR and are used for the expanded and improved GBF processing. The following main modifications were included in the routine processing:

The detector upgrade for 6 arrays

Natural seismicity in particular can produce S onsets with relatively small radiated SV energy and the more energetic radiated SH component is more difficult to detect on vertical sensors. Therefore the concept of coherent horizontal beams was developed and extensively tested for regional arrays with more than one 3-component sensor (Schweitzer, 1994). Such detection beams have been implemented for three regional arrays (ARCES, GERES, and NORES). This significantly increased the number of S-phase observations.

The optimized detector recipes for the Spitsbergen array SPITS (Schweitzer, 1998) were developed with special consideration for the low velocities in the sediments below the array. In addition, the high local seismicity due to movements in nearby glaciers and mining induced seismicity required a set of beams with very low velocities. These improvements were necessary before SPITS could be used in the GBF process.

Based on the experience with SPITS, similar detection recipes were developed for the Apatity array (APA) and Hagfors (HFS), and implemented in the automatic processing.

The f-k analysis upgrade

After upgrading the detectors for 6 out of 7 regional arrays, the automatic parameter extraction for each detected onset was also changed and improved. Based on experience gained from the four classical regional arrays ARCES, FINES, GERES, and NORES (Schweitzer, 1994), the f-k analysis recipes were optimized for each array individually. Most important was the development of an algorithm to find an optimal length and the best positioning of the time window used for the f-k analysis.

For GERES, and more importantly for SPITS, it became helpful to correct for elevation differences within the array site during the f-k analysis. The correction for elevation differences was also useful for beamforming prior to measuring the amplitude of the onset.

The numerous Pg and Rg observations at SPITS require additional data processing. The problem is that we observe an overlap between the apparent velocities of Pg and Sn, and that we observe very small apparent velocities for Rg onsets from events at close distances. These Rg phases can be erroneously interpreted because they tend to produce large energy at the side lobes of the SPITS array transfer function. Following the experience with similar effects for the Matsushiro array (MJAR) in Japan (Schweitzer, 1997), a widely optimized set of rules with several f-k analyses for the same detection was developed to estimate apparent velocities and back-azimuths at SPITS (Schweitzer, 1998).

The experiences with these arrays were also used to optimize the signal processing for APA and HFS, so that since 10 April 1999 all regional array data at NORSAR are analyzed with the new processing algorithms.

Preprocessing of detection data

To detect both the P- and S-phases from very local events (within 30 km of the arrays), we have changed the detector recipes for APA, HFS, and SPITS, such that detections now can be reported with time differences down to 0.5 seconds. A side effect of this is an increased number of detections in the coda of regional and teleseismic events. To reduce the number of coda detections, the preprocessor first merges detections that are very close in time (within 2 seconds) and that have similar slowness estimates (azimuth and apparent velocity).

In order to avoid false phase associations by the GBF method, it is important to place restrictions on the use of detected signals. E.g., if the f-k analysis of a given signal at ARCES results in a confident apparent velocity estimate of 7.2 km/s, we can assume that this is not a teleseismic P or a regional S-type phase (Sn, Lg, Rg). If the phase possibly is a Pg, we will restrict the corresponding event location to a 0 to 600 km distance interval from the array. In case the phase is a Pn, we will only allow the event to be located between 160 and 1300 km from the station. The relations between apparent velocity estimates and distance limits of the different phases are obtained from analysis of well-defined events. In addition, the estimated azimuths put additional restrictions on the use of the detected signal in the GBF. E. g., for ARCES we currently do not allow the events to be located outside a sector of ±25 degrees around the esti-

mated azimuth. For each detection, the distance and azimuth limits for a given list of phases (P, Pn, Pg, Sn, Lg, Rg) are stored in a database for use by GBF.

For each array are also attempt to group arrivals which are likely to originate from the same local or regional event. In short, we first search the detection list for phases with typical Pn/Pg apparent velocity estimates. If within a relatively short time interval (~40 seconds), phases are found with S-type apparent velocity estimates, and with comparable azimuths, we assign the phases to the same event. Based on the time difference between the first P and the first S of the group, we are calculating an approximate distance to the event. In the subsequent GBF process the phases in this group can only be associated with events close to the approximate initial location.

As a final preprocessing step we group together subsequent phases with typical teleseismic apparent velocity estimates. The automatic detector often reports several detections within 10-20 seconds after the first teleseismic P, and these coda detections will not be used as defining phases by the GBF process.

The ORACLE database previously used for storing the results from the preprocessor has been replaced by a set of ASCII files. For each station, there is a "circular" database file, an index file, a "control" file, and a set of timestamp files. The number of arrivals which can be held in the circular file is decided by the user and listed in the control file.

The new preprocessor software has been written in C to replace the old FORTRAN routines and consists of two main modules:

phasescan This program reads the files with the arrival parameters (FKX files), merges arrivals as necessary, and writes new FKX files. The velocities and azimuths of the possibly merged arrivals are compared to a table of rules governing the initial distance estimates, and the results are written to the ASCII "database" for that station.

eventscan This module identifies and updates distance limits for groups of arrivals satisfying the input criteria given in a parameter file. The program is executed three times, first for local events, second for regional events, and finally for the coda of teleseismic events. Arrivals will not be flagged multiple times (*e.g.*, if a set of arrivals is flagged as local, they will not be considered when scanning for regional or teleseismic events).

Rules for determining initial distances for arrivals at Spitsbergen

The GBF preprocessor uses a standard set of tables for estimating the initial distance limits which depend on the apparent velocity estimate alone. However, the observed apparent velocities (and azimuths) are dependent on the actual propagation path between source and receiver (*e.g.*, Schweitzer and Kværna, 1995).

In the case of the SPITS array, large slowness variations are observed, and we initially tried to accommodate these variations with a simple approach. The Pn apparent velocity estimates from a set of manually located SPITS events are shown in Fig. 6.3.1. We see distinctly higher velocities to the northeast, and predominantly low velocities in the southwest. After obtaining geologic information of the crust below the SPITS array (see Fig. 6.3.2), we can explain parts

of the effect by dipping sedimentary layers in the uppermost crust. After binning the Pn data in distance and azimuth, a function of the form

$$v = const + f_1 \cdot \Delta + f_2 \cdot \sin(azi + \phi)$$

was fit to the velocities (see Fig. 6.3.3). The value of $\pm 1.5\sigma$ was used as a guideline for deciding velocity limits as a function of azimuth for this phase. The phases Pg, Sn, and Lg show similar patterns and we have for these phases also derived velocity versus azimuth functions.

Coverage of the regional grid system

An input parameter to the GBF algorithm is the grid system of possible event locations. For each grid point, the detection logs of the different arrays are searched for signals matching the predicted travel time, azimuth and slowness of phases originating at the grid point. When a given number of matching phases are found, initial event hypotheses are formed. A denser grid system is then constructed around the grid point providing the largest number of matching phases, and the data are reprocessed for a shorter time interval around the initial origin time.

The coverage and density of the "old" grid system used up to April 1999 is shown in Fig.6.3.4. Also shown are the locations of the arrays used in the GBF processing. The grid nodes are deployed across latitude circles with a distance of 1.5 degrees. Notice the distortion of the grid system in the vicinity of the North Pole. As an example, Fig. 6.3.5 shows the denser grid system constructed around an initial event location in the Kara Sea. The distance between the grid nodes is 0.3 degrees.

In addition to including the SPITS array in the GBF processing, we also needed a more complete grid coverage in the polar region. The gridding algorithm was modified, and the result is shown in Fig. 6.3.6. The distance between the nodes of the coarse grid system is still 1.5 degrees, and the coverage is extended. The new denser and enlarged grid system constructed around the initial event location is shown in Fig. 6.3.7, where the distance between the grid nodes is reduced to 0.2 degrees.

A preliminary evaluation of results from the new GBF process

For comparing the results of the "old" and the "new" GBF processing, data from a 59 day time period from 15 February to 14 April 1999 were processed using both setups. Different from the "old" setup, the "new" GBF included data from the SPITS array, improved detector and f-k recipes, enhanced preprocessor functionality and parameters, an enlarged and more uniform grid system, and a "cleaned" GBF code. In Fig. 6.3.8 we show locations of all events from both runs. Notice in particular the increased number of events in the Arctic region north of 70° latitude, and outside the coverage of the "old" GBF grid system. For the "new" GBF, the events close to the North pole exhibit a "suspicious" geometric pattern. We think that this may be a boundary effect of the parameter setting, and we will further investigate this problem.

All methods for automatic phase association produce false event definitions, but we have not in this first evaluation assessed the false alarm rate of the two runs. In order to sort out possible false event definitions we have in Fig. 6.3.9 plotted events which have at least one station with defining P and S phases, and at least one additional station with a defining P-phase. Particularly striking is the large number of events along the mid-Atlantic ridge system for the "new" GBF.

In Fig, 6.3.10 we have plotted events with at least 3 defining P-phases (from three different stations). This is a criterion similar to that used for defining events at the Prototype International Data Center (PIDC) in Arlington, USA. For the "old" GBF, notice the grid boundary effect in the Mediterranean Sea and some "suspicious" alignments to the west of the Black Sea. For the "new" GBF, there is a better definition of the seismicity along the mid-Atlantic ridge, combined with a visually better clustering of the events at the mining areas in northern Europe. The "new" GBF produces an increased number of events scattered around the Russian territory. We believe that a portion of these may be false phase associations, particularly caused by the new detections at the SPITS array.

Finally, we show in Fig. 6.3.11 the events reported in the Reviewed Event Bulletin (REB) of the PIDC, and the events reported by NEIC for the same time period. Up to 18 March NEIC events are those reported in the weekly bulletins, but after that time only the Quick Epicenter Determinations (QED) were available. When comparing the REB events to the "new" GBF events with at least 3 defining P-phases (see Fig. 6.3.10), it seems that the "new" GBF has captured most of the events reported in the REB. Notice in particular the events located along the mid-Atlantic ridge, in the Mediterranean, and in the Caucasus.

The NEIC events of Fig. 6.3.11 show a very different pattern. Only the largest events along the mid-Atlantic ridge are reported, and no events are reported from Fennoscandia, the Baltic states, or Russia. Due to extensive and timely reporting from many local networks in southern Europe to NEIC, the bulletin has a very good coverage for this region.

Conclusion

Our preliminary assessment of the "new" GBF processing, now including the SPITS array, is that it provides a significant improvement with respect to monitoring of the European Arctic. Because of the less restrictive phase definition criteria, the "new" GBF outperforms the PIDC REB in the regional distance regime from the arrays. However, we need to assess in more detail the false alarm rate and methods to avoid erroneous phase associations.

After updating the recipes for detection and f-k analysis for all regional arrays, the "new" GBF processing was set into operation on 10 April 1999. The operational stability of the "new" GBF is significantly improved compared to the "old". As a rule we have available an automatic network bulletin within 1 - 1 1/2 hours after real time. The results are made available to the public at the NORSAR Web pages
(**http://www.norsar.no**).

T. Kværna
J. Schweitzer
L. Taylor
F. Ringdal

References

Ringdal, F. and T. Kværna (1989). A multi-channel processing approach to real time network detection, phase association, and threshold monitoring. Bull. Seism. Soc. Am. **79**, No. 6, pp. 1927-1940.

Schweitzer, J. (1994). Some improvements of the detector / SigPro - system at NORSAR. In: NORSAR Semiannual Tech. Summ. 1 October 1993 - 31 March 1994, NORSAR Sci. Rep. 2-93/94, Kjeller, Norway, 158-163.

Schweitzer, J. (1997). Recommendations for improvements in the PIDC processing of Matsushiro (MJAR) array data. In: NORSAR Semiannual Tech. Summ. 1 April - 30 September 1997, NORSAR Sci. Rep. 1-97/98, Kjeller, Norway, 128-141.

Schweitzer, J. (1998). Tuning the automatic data processing for the Spitsbergen array (SPITS). In: NORSAR Semiannual Tech. Summ. 1 April - 30 September 1998, NORSAR Sci. Rep. 1-98/99, Kjeller, Norway, 110-125.

Schweitzer, J and T. Kværna. (1995). Mapping of azimuth anaomalies from array observations. In: NORSAR Semiannual Tech. Summ. 1 October 1994 - 31 March 1995, NORSAR Sci. Rep. 2-94/95, Kjeller, Norway, 99-106.

Sigmond, E. M. O. (1992). Bedrock map, Norway and adjacent ocean areas. Geologiske Undersøkelse 1986-1992.

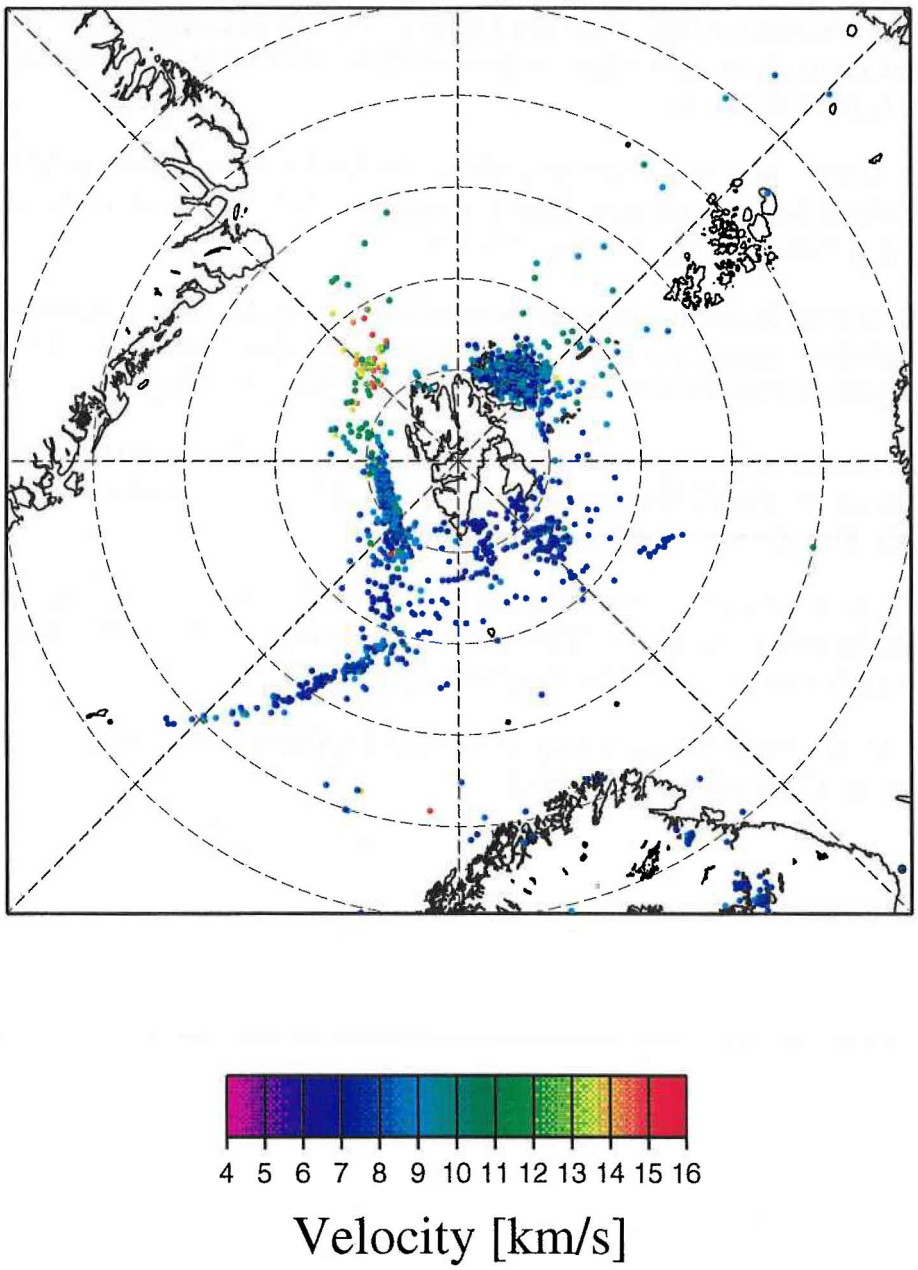

Figure 6.3.1. Pn apparent velocity estimates for a set of manually located SPITS events.

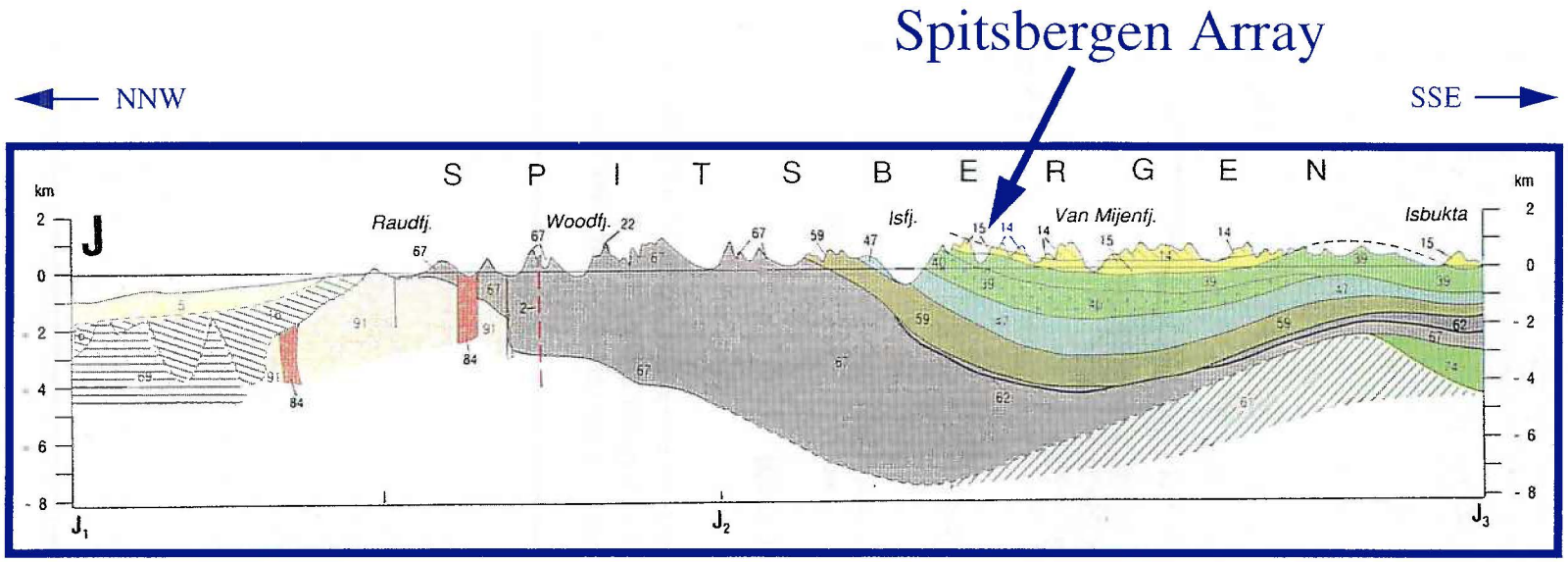

Fig. 6.3.2. Geological cross-section through the uppermost crust below the SPITS array. Modified after E.M.O. Sigmond, 1992.

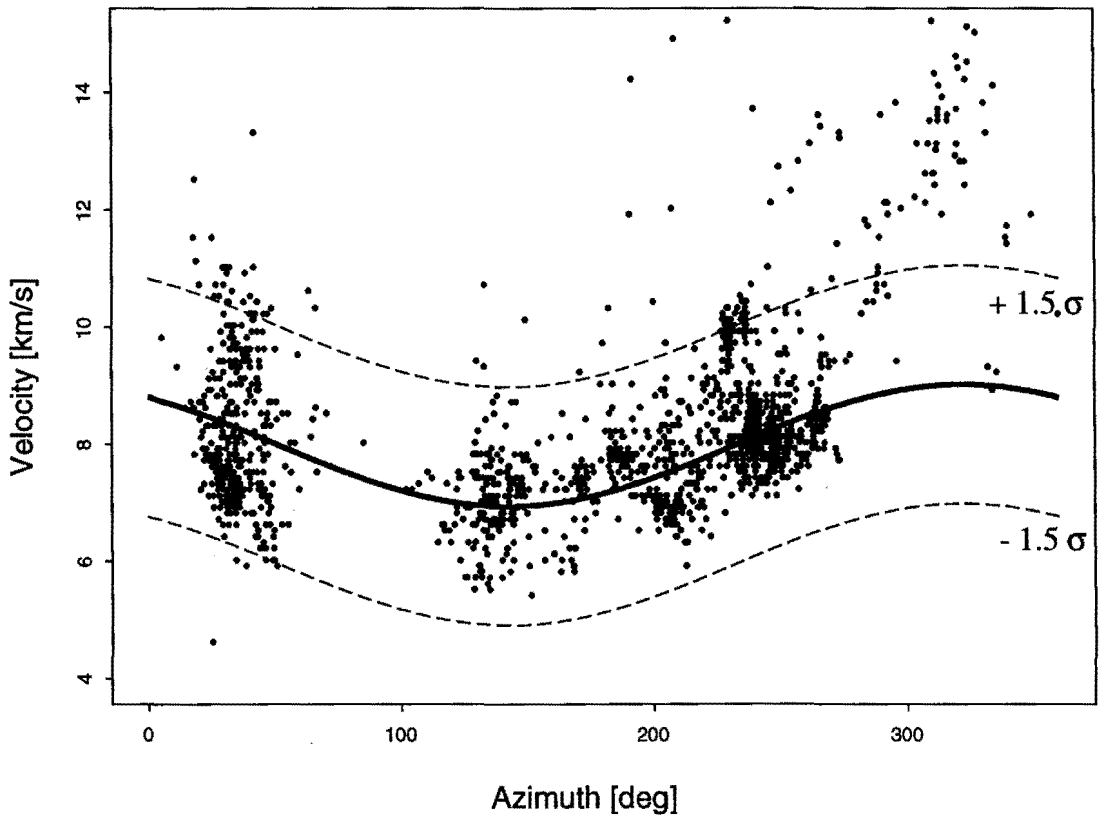

Fig. 6.3.3. Plot of Pn apparent velocities of Fig. 6.3.1 versus azimuth at the SPITS array. After binning the Pn data in distance and azimuth, a function of the form $v = const + f_1 \cdot \Delta + f_2 \cdot \sin(azi + \phi)$ *was fit to the velocities. The lines showing the* $\pm 1.5\sigma$ *are also shown.*

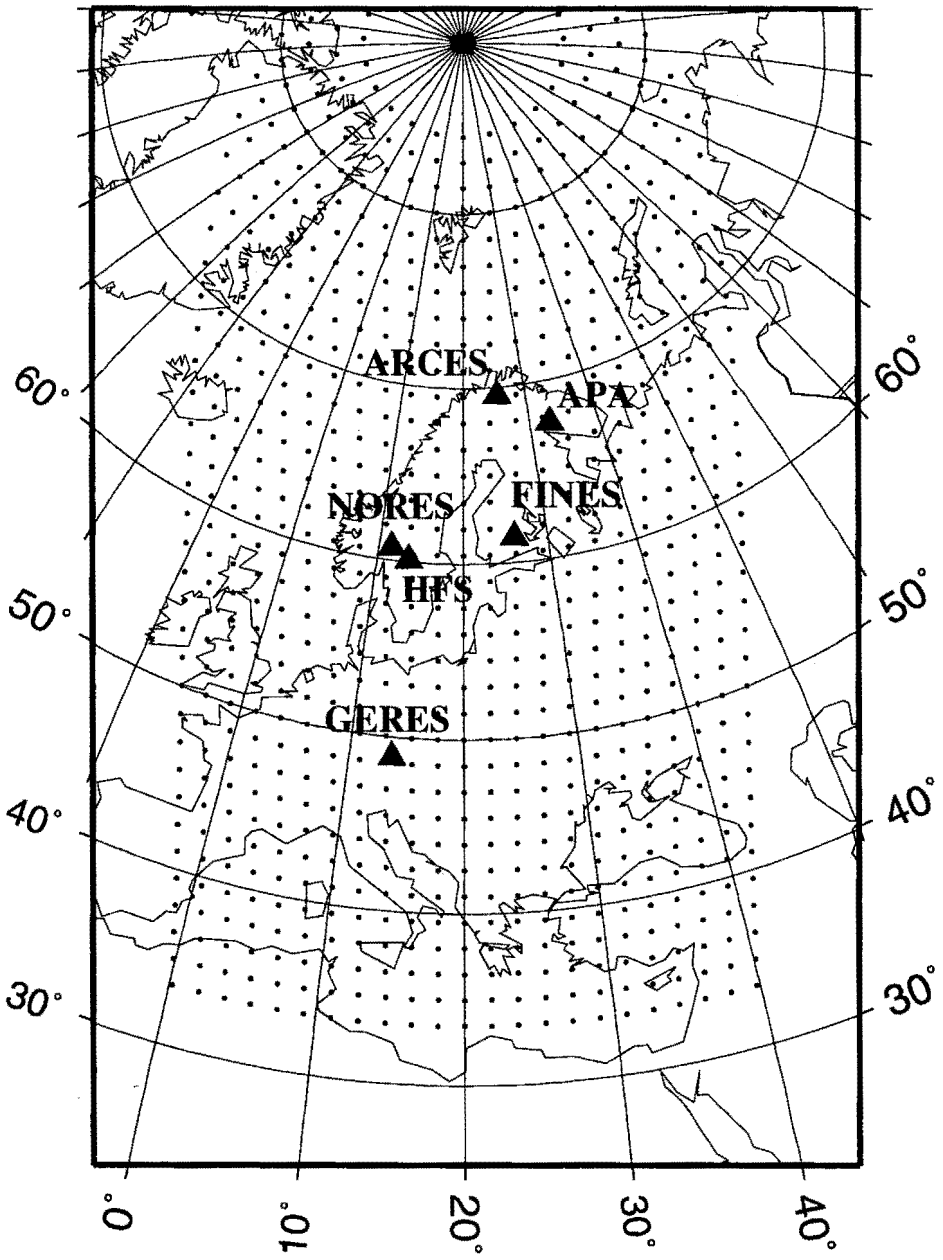

Fig. 6.3.4. This map shows the stations processed and the initial grid system used by the "old" GBF. The distance between the grid nodes is 1.5 degrees.

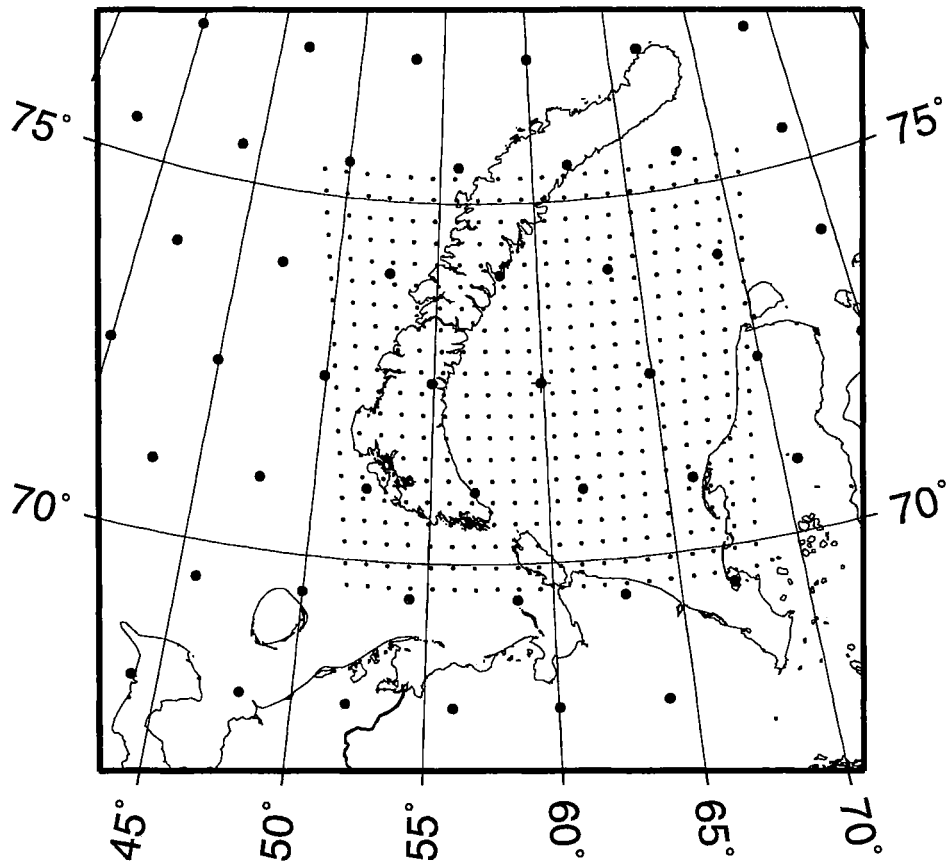

Fig. 6.3.5. Map of the denser grid system used by the "old" GBF, in this case constructed around an initial event location in the Kara Sea. The distance between the grid nodes is 0.3 degrees.

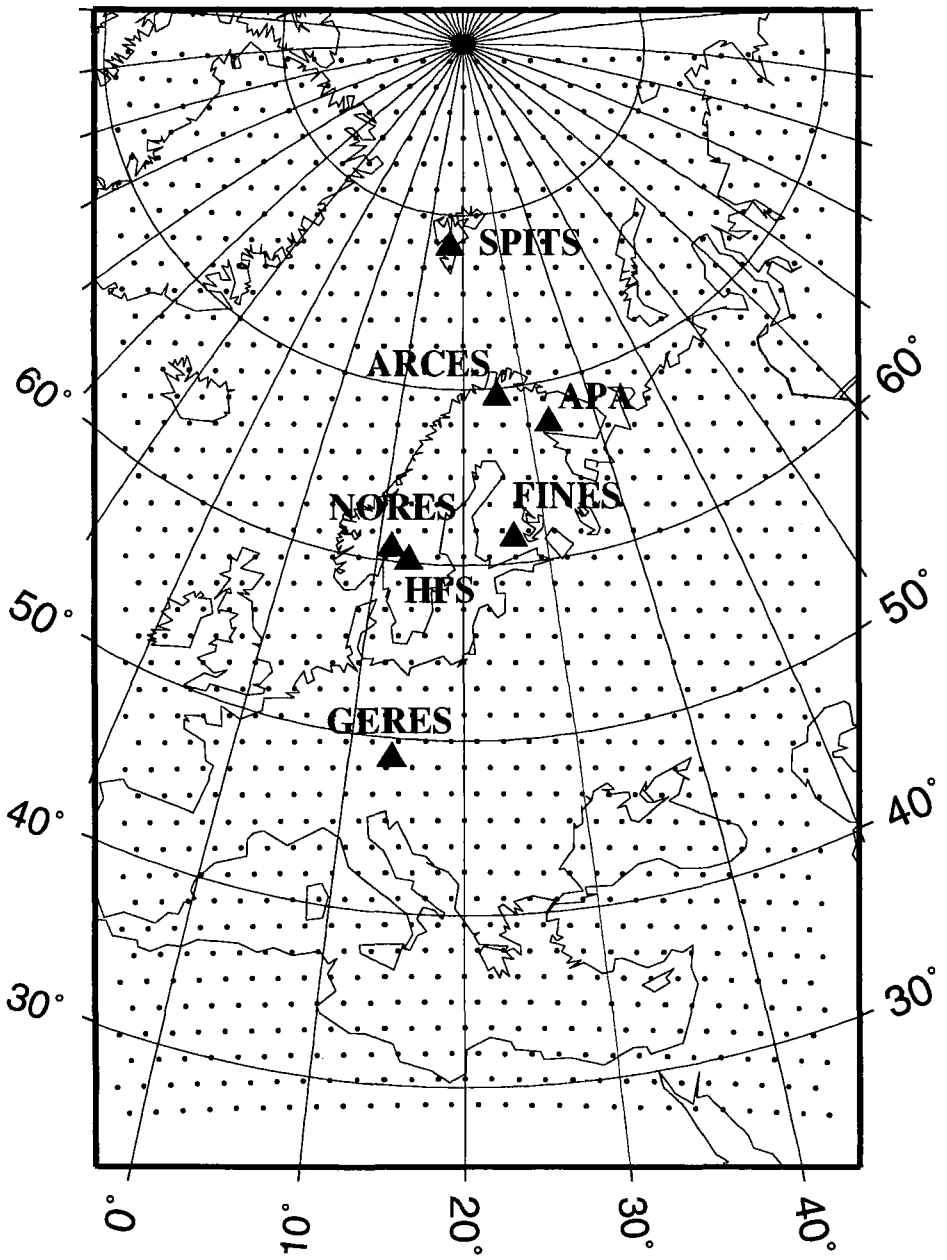

Fig. 6.3.6. This map shows the stations processed and the initial grid system used by the "new" GBF. The distance between the grid nodes is 1.5 degrees.

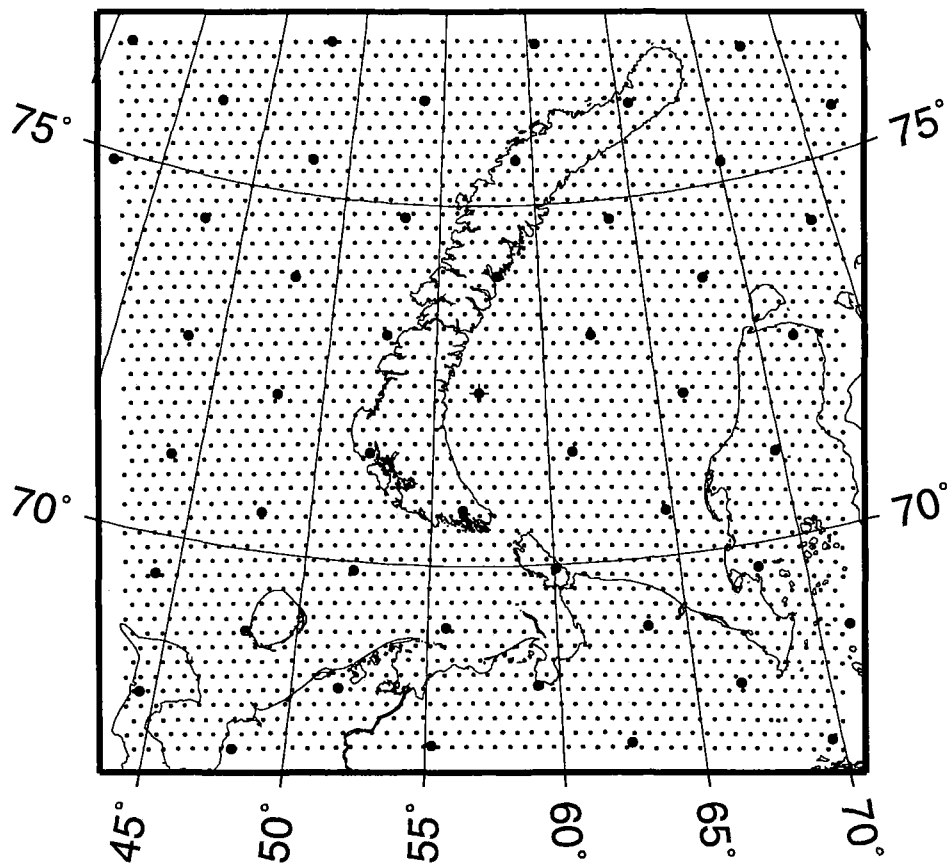

Fig. 6.3.7. Map of the denser grid system used by the "new" GBF, in this case constructed around an initial event location in the Kara Sea. The distance between the grid nodes is now 0.2 degrees.

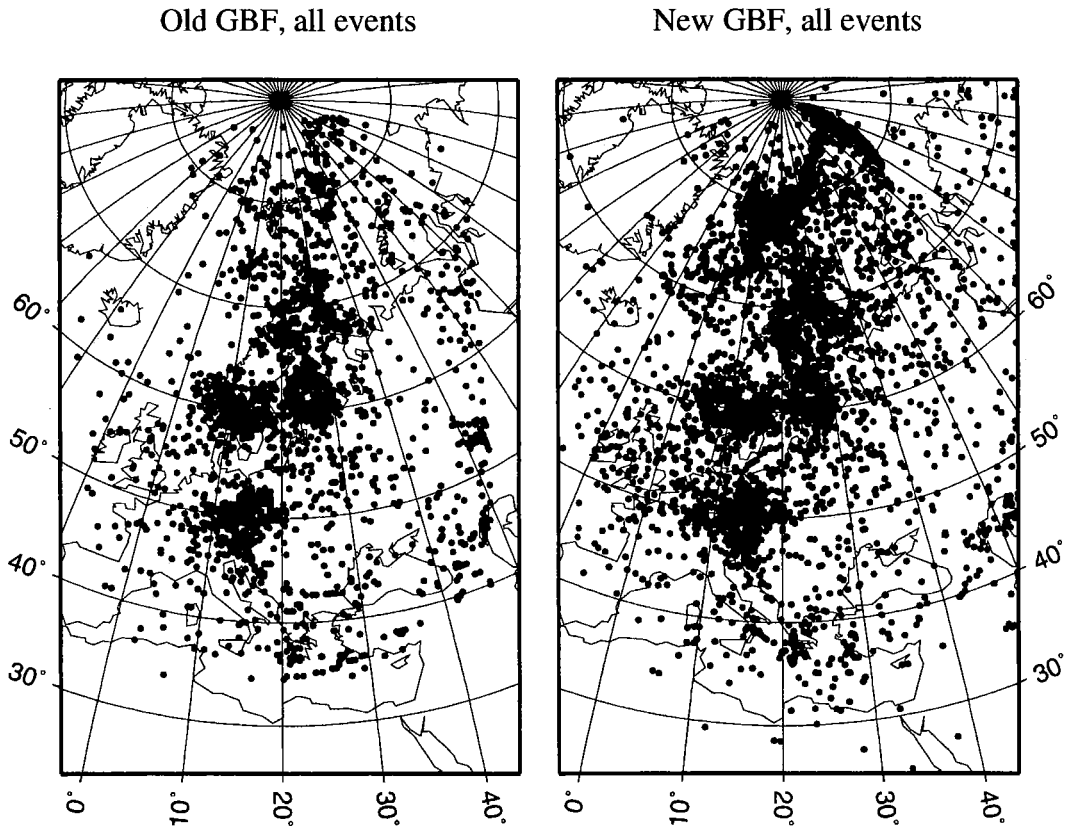

Fig. 6.3.8. Maps of all events defined by the "old" and the "new" GBF version after processing data from the time period from 15 February to 14 April 1999.

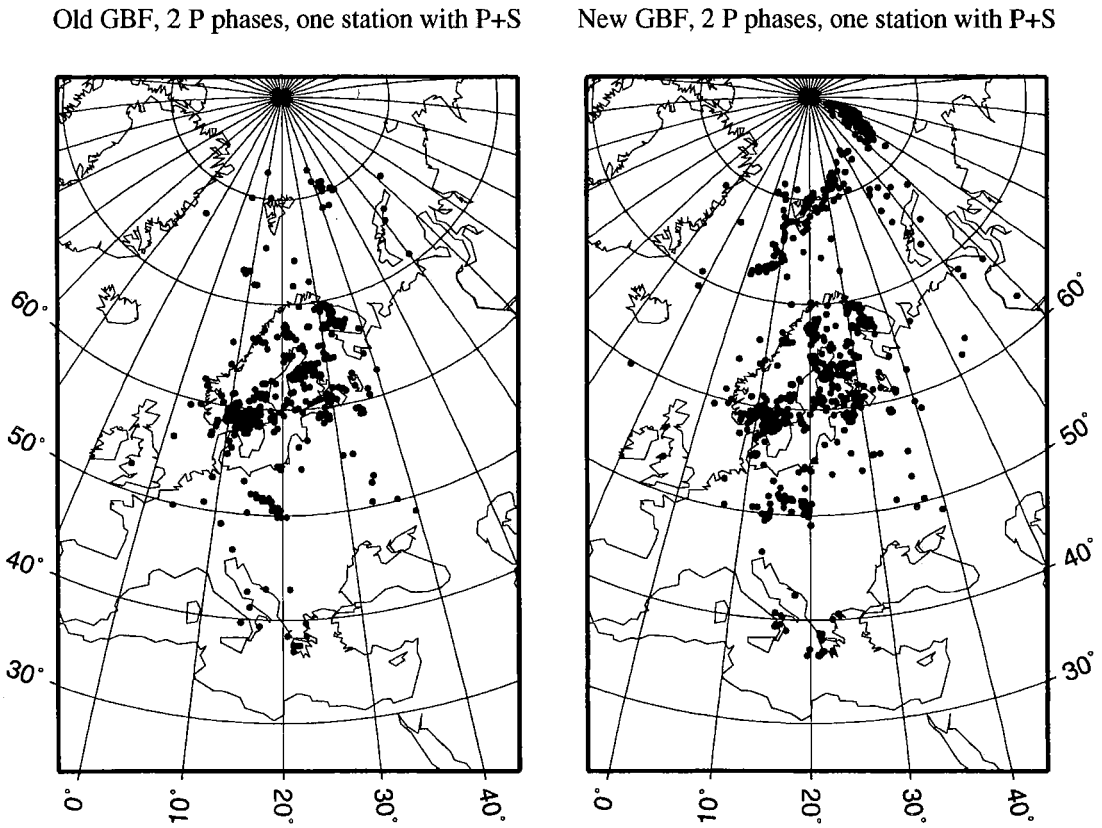

Fig. 6.3.9. Maps of events defined by the "old" and the "new" GBF processing which have at least one station with defining P and S phases, and at least one additional station with a defining P. The processed data are from the time period from 15 February to 14 April 1999.

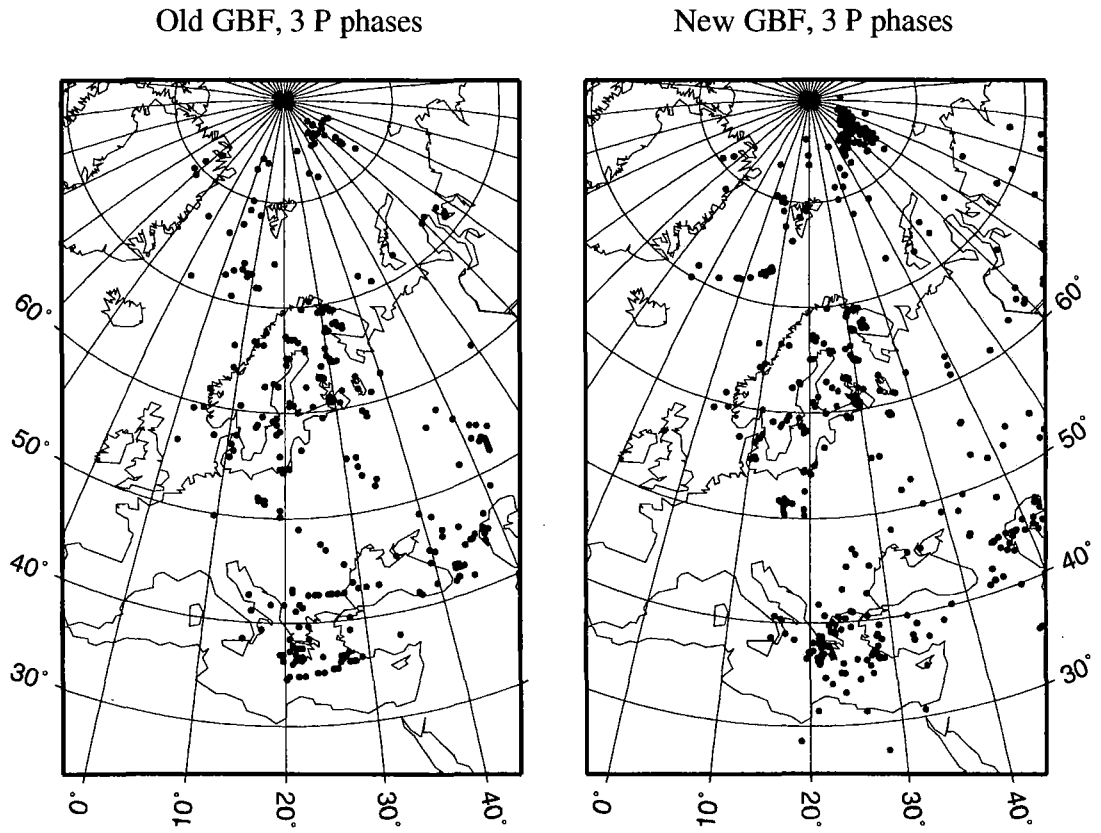

Fig. 6.3.10. Maps of events defined by the "old" and the "new" GBF processing which have at least 3 defining P-phases (from three different stations). The processed data are from the time period from 15 February to 14 April 1999.

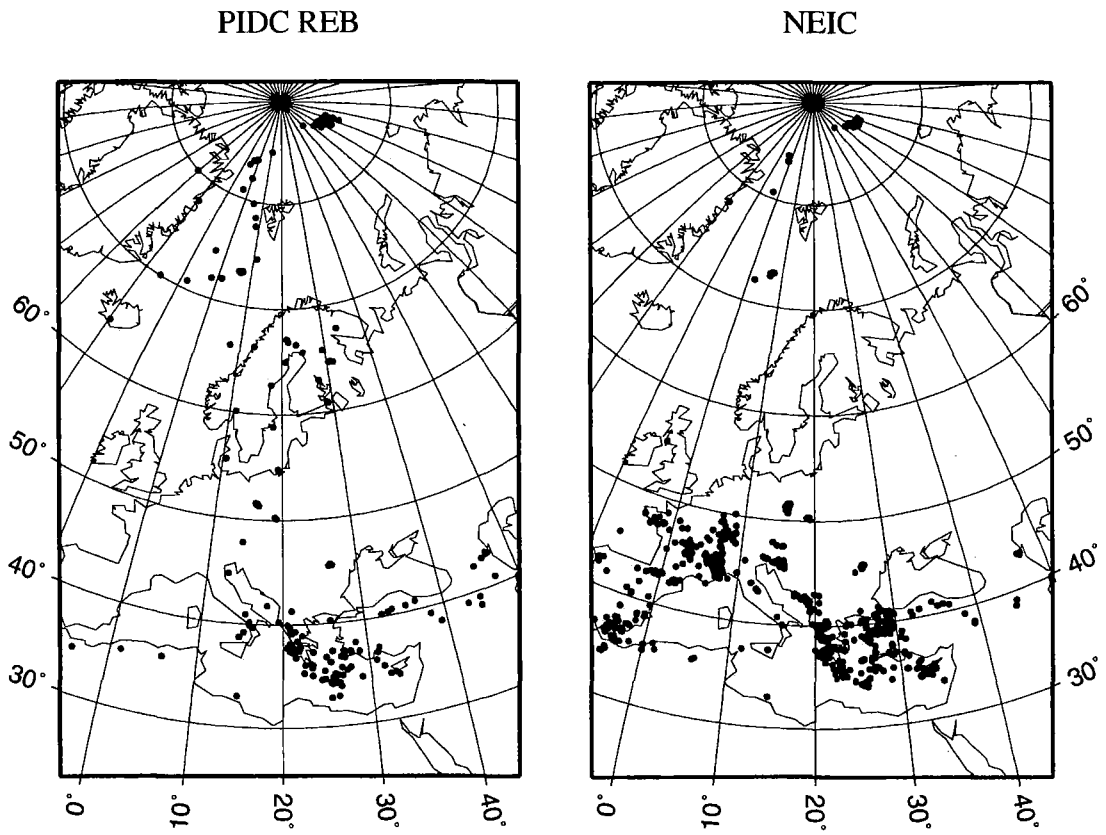

Fig. 6.3.11. These maps show the events reported in the Reviewed Event Bulletin (REB) of the PIDC, and the events reported by the NEIC for the time period from 15 February to 14 April 1999. Up to 18 March NEIC events are those reported in the weekly bulletins, but after that time only the Quick Epicenter Determinations (QED) were available.